PROGRESS IN COLOR, COLORANTS AND COATINGS

available online @ www.pccc.icrc.ac.ir

Prog. Color Colorants Coat. 11 (2018), 209-220

Ministry of Science, Research and Technology
Institute for Color Science and Technology

Synthesis, Characterization and Investigation of Photocatalytic Activity of Transition Metal-doped TiO_2 Nanostructures

M. Hosseini-Zori*[1], Z. Mokhtari shourijeh[2]

[1.] Department of Inorganic Pigments and Glazes, Institute for Color Science and Technology, P.O. Box: 16765-654, Tehran, Iran.

[2.] Department of Environmental Research, Institute for Color Science and Technology, P.O. Box: 16765-654, Tehran, Iran.

ARTICLE INFO

Article history:
Received: 13 Jul 2018
Final Revised: 15 Oct 2018
Accepted: 21 Oct 2018
Available online: 11 Nov 2018

Keywords:
Doping
TiO_2
Photocatalyst
Reverse Microemulsion
Nanostructure.

ABSTRACT

In this work, M-doped TiO_2 nanostructures (M: Fe, Co and Ni) were synthesized by reverse microemulsion method. The as-prepared products were analyzed by different techniques such as scanning electron microscopy (SEM), Transmission electron microscopy (TEM), X-ray diffraction (XRD) and Fourier Transform Infrared Spectroscopy (FT-IR). The effect of various dopants (Fe, Co and Ni) on band gap and photocatalytic properties of TiO_2 was investigated. The decolorization abilities of the as-prepared M-TiO_2 nanostructures (M = Fe, Co and Ni) under UV and visible irradiation were investigated using three dyes: Acid Red 1, Reactive Blue 21 and Indigo Carmine. The role of pH value and reaction time on photocatalytic performance of products was also studied. The results showed that the degradation of dyes in lower pH is more and photocatalytic performance Fe-doped TiO_2 is better than the others. Kinetic investigation of the photodegradation illustrated reactions were following the Langmuir-Hinshelwood mechanism. Prog. Color Colorants Coat. 11 (2018), 209-220© Institute for Color Science and Technology.

1. Introduction

Dyes and pigments are widely applied in various industries such as textiles, paper, rubber and plastics, but often create severe environmental pollutions. In addition, the consumption of dyes and pigments impress the quality of life by causing health problems like reproductive, developmental, neuron and acute toxicity [1-4]. By considering the volume and chemical composition of the wastewater discharge, technologies and methods that can remove or decrease these pollutants have been extensively received considerable attention in recent years. The treatment of waste water in recent years. Various technologies are used for waste water treatment such as biological oxidation, physical-chemical, ozonation, chemical precipitation and electrocoagulation, each of them has limitations and advantages. For instance, most physicochemical dye removal methods are expensive and greatly interfered by other wastewater constituents andthey have limited versatility [2]. Recently, semiconductors are used as photocatalysts for the removal of organic and inorganic species from aqueous or gas phase [1, 5-8].

Among the various photocatalysts, TiO_2 has been investigated because of its properties such as low cost,

*Corresponding author: mhosseini@icrc.ac.ir

readily available, nontoxic and excellent stability and anticorrosion [12, 13] various applications in many fields such as photovoltaic cells, batteries, chemical sensing [9], optical emissions, photonic crystals, catalysis, photocatalysis [10] and environmental purification [11].

In recent years, scientists tried to enhance photoactivity in both ultraviolet and visible light. Since TiO_2 has a large band gap (3.2 eV), its photocatalytic activity is in the range of UV irradiation. Hence, considerable efforts have been made to reduce band gap including TiO_2 coupling with other semiconductors having narrow band gap, combining noble metals with TiO_2, and TiO_2 doping with metal and nonmetal elements. The results showed that the doping of metal ions such as Ni^{2+} [14], Fe^{3+} [15] and nonmetal ions such as N^{3-} [16], F^- [17] in TiO_2 lattice has improved photocatalytic activity by trapping photo-generated electrons. Ranjitha et al. modified TiO_2 nanoparticles utilizing Ni^{2+} ionby sol-gel coating method. Their successful attempts caused improvement ofphotocatalyst activity of TiO_2 under visible light [18]. In addition, Zhao et al. prepared mixed phase Co^{2+}-doped TiO_2 and they could decrease adsorption edge into the visible region [19]. Gupta et al. prepared modified $CoFe_2O_4$@TiO_2 particles mounted on reduced graphene oxide [20] and investigated the removal performance of terephthalic acid under UV illumination by Ag/TiO_2 catalyst. Almeida et al. reported 98.8% degradation performance in an optimum condition [21]. At this study, M-doped TiO_2 (M = Fe, Co and Ni) nanostructures were synthesized by reverse microemulsion. The products were characterized by SEM, FT-IR, TEM and XRD methods. The photocatalytic performance of products under UV and visible irradiation were studied by degradation of three dyes: Acid blue 74 (Indigo carmine), Acid red 1, and Reactive blue 21 dyes. The effect of various parameters, including the photocatalyst dosage, dye concentration, pH, and time were investigated. The results showed that the photocatalytic activity of products in acidic environmental is better than the others. The performance of products was compared and the results illustrated that Fe-TiO_2 is more active than the others. Kinetic investigation of the photo-degradation illustrated reactions were following the Langmuir-Hinshelwood mechanism.

2. Experimental

2.1. Characterization

Titanium tetraisopropoxide (TTIP, > 99%) and 1-Hexanol (>99% obtained from Merck, code8. 04393. 1000) were obtained from Sigma-Aldrich. Iron sulfate (1.03965.0500), Cobalt sulfate (1.02546.1000) and nickel sulfate (1.06727.1000) were obtained from MERCK. Three industrial dyes, i.e. Acid Red 1 (A.R.1), Reactive Blue 21 (R.B.21) and Acid blue 74 (A.B.74), which were used as organic pollutants, were purchased from Isfahan Polyacryl Inc. Hydrochloric acid (HCl) and Sodium hydroxide (NaOH) were supplied by Merck Co. The chemical structures and main characteristics of the dyes are shown in Figure 1 and Table 1, respectively.

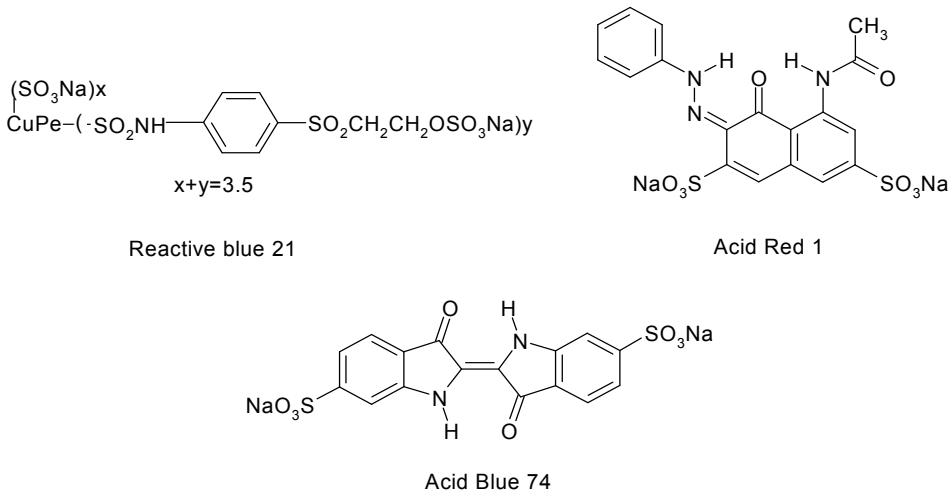

Figure 1: The chemical structure of the dyes.

Table 1: Main characteristics of the dyes.

Name	Molecular Formula	Molecular Weight	Molecular Structure	λ_{max}	Code
Acid red 1	$C_{18}H_{13}N_3Na_2O_8S_2$	509.42	Single azo class	544	AR1
Reactive blue21	$C_{18}H_{15}N_7OS$	377.43	Phthalocyanine class	663	RB21
Acid blue 74	$C_{16}H_8N_2Na_2O_8S_2$	466.36	Indigo class	610	AB74

The XRD patterns of products was recorded by a Rigaku D-max C III XRD using Ni-filtered Cu Kα radiation. SEM and TEM images were obtained on Philips CM120. UV-visible absorption spectra were also measured by a Cecil CE9200 spectrophotometer. The TUV 15W SLV/25 was used as the source of UV irradiation to perform photocatalytic tests. It was obtained from Philips lighting company. Fourier transform infrared (FT-IR) spectrometer (Equinox 55, from Bruker; Germany) was used to analyze the chemical and/or physical interactions over the wave number range of 450 – 4000 cm^{-1}. Diffuse reflectance spectra were taken using a scanning UV–vis spectrophotometer (CECIEL 2021).

2.2. Preparation of pure TiO_2 and M-doped TiO_2 (M = Fe, Co and Ni) nanostructures

CTAB, as a surfactant, and iso-octane, as a continuous phase (precursor), were added to the solution to produce microemulsion reaction medium. Afterwards, 0.2 M CTAB is dissolved in the organic solvents under ultrasonic stirring, and then a sufficient amount of TTIP was added to the microemulsion solution, resulting in the formation of thermodynamically stable reverse micelles, containing a hydrophilic core, categorized in the hydrophilic head group extracted from the substance CTAB, and a hydrophobic alkyl tail, extending into the nonpolar continuous phase solvent (precursor). After preparation of TiO_2 seed nanoparticles in reverse microemulsions, depending on what dopant was produced, Iron Sulfate, Cobalt Sulfate or Nickel Sulfate was dissolved in a sufficient amount of water and added drop-wise into the microemulsion. The particle size was dependent on the droplet size of microemulsion. The stability of the emulsion was directly affected by water to surfactant ratio. In this work, this ratio for all the experiments was fixed at 2. According to former work, excess water may result in instability of emulsion [22]. In other words, the eventual particles size depended on the size of the microemulsion droplets. The doped TiO_2 was prepared based on calculating the formula, as shown in Table 2. For example, Iron-doped titania ultrafine particles was coded as TiO_2-Fe and it was prepared based on the following formula:

1 TiO_2-0.02 Fe into the microemulsion solution. Then, 15 mL water and 15 mL ethanol were added to 25 mL of the microemulsion solution, so the solution was separated into two phases. The obtained gel, extracted from the lower phase of solution, was dried at 100 °C for 1 h. The resulted powder was calcined at 300 and 500 °C for 1 h. Then, the obtained product was collected and characterized by various techniques.

2.3. Photocatalysis experiments

The photocatalytic activity of M-doped TiO_2 nanostructures (M = Fe, Co and Ni) were evaluated by photocatalytic decolorization of dyes into a batch photoreactor (light source: a UV lamp of 15 W or visible irradiation) containing 0.03 g photocatalyst into 1000 mL of 20 mg/L dye. The mixture was aerated for 30 min to reach adsorption equilibrium. Next, the mixture was placed inside the photoreactor in that the vessel was 15 cm away from the UV source (mercury lamp). Photocatalytic tests were done at room temperature. The mixtures were exposed to radiation for certain times and then analyzed by UV-vis spectrometer. The effects of pH and time on photocatalytic performance of products were studied. The effect of each parameter was investigated by keeping the other parameters constant. The equation used to calculate the dye decolorization efficiency in the treatment experiments is as follows:

$$DEC\% = \left(1 - C/C_0\right) \times 100 \quad (1)$$

In this equation C_0 and C are the initial and present concentrations of the dye in solution (ppm), respectively [23].

3. Results and Discussion

3.1. XRD pattern

Figure 2 depicts the XRD patterns of heat-treated M-doped TiO_2 (M = Fe, Co and Ni) at 350 °C. At this temperature, the formation of anatase phase was confirmed for all the samples. According to the results, it should be said that the gels obtained from microemulsion method were amorphous and the formation of anatase phase occurs at about 300 °C. On the other word, increasing the calcination temperature increases the crystallinity and particle size of the products [24].

3.2. TEM and SEM images

In Figure 3, TEM images of M-doped TiO_2 (M = Fe, Co and Ni) nanostructures prepared at 350 °C are shown. The particles have spherical shape with uniform size distribution about 40-50 nm. The formation of agglomerated secondary particles in the samples calcined at 300 °C is clearly observed in Figure 4.

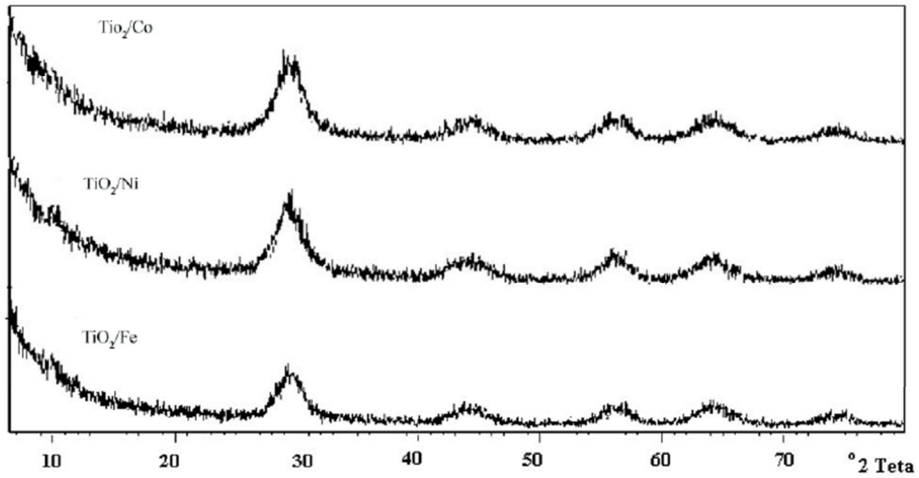

Figure 2. XRD patterns of TiO_2-Fe, TiO_2-Ni, and TiO_2-Co.

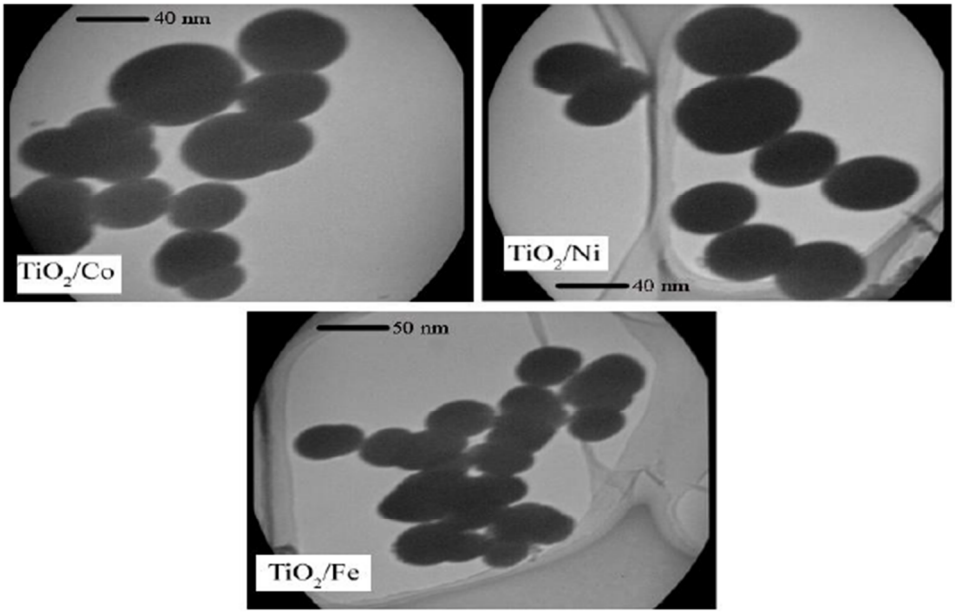

Figure 3: TEM images of TiO_2-Fe, TiO_2-Ni and TiO_2-Co after calcination at 300 °C.

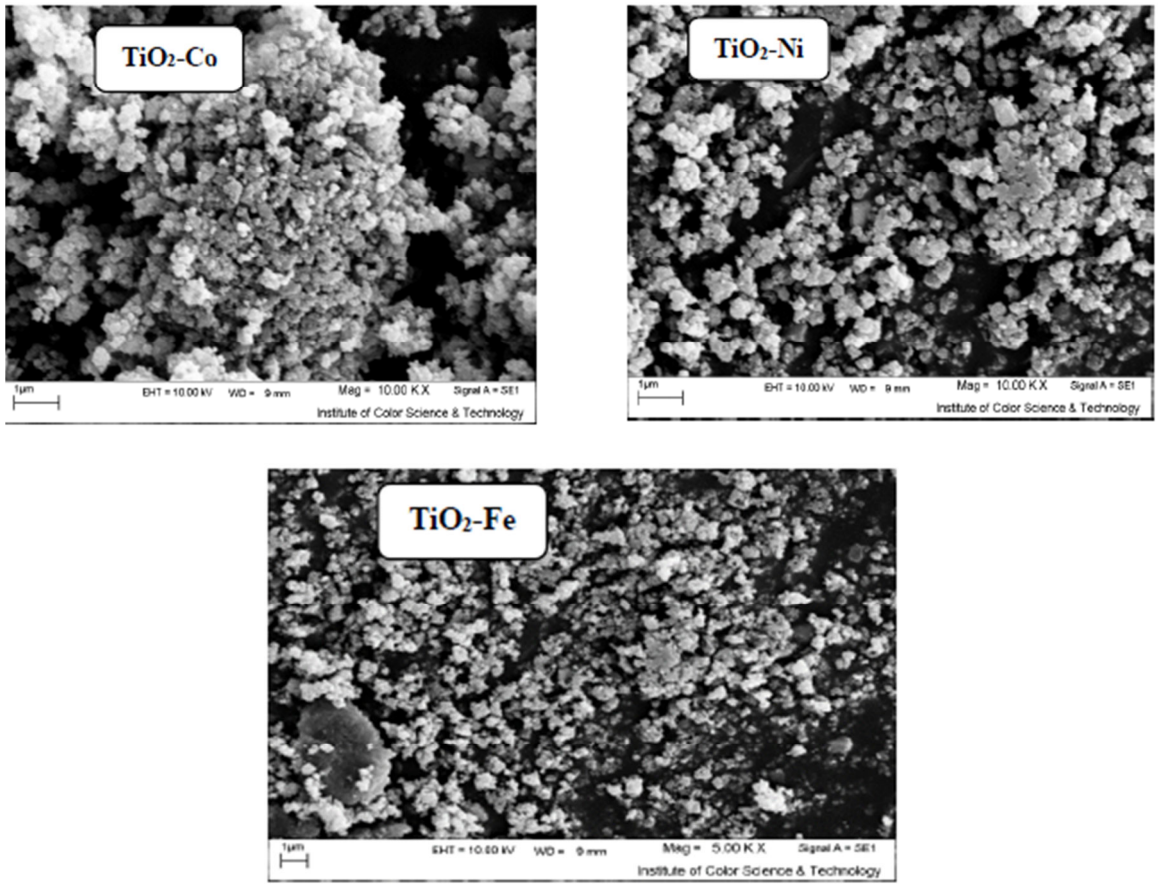

Figure 4: SEM images of TiO_2-Fe, TiO_2-Ni and TiO_2-Co after calcination at 300 °C.

These samples contain shrinkage and inter crystal pores. It was very difficult to verify the primary particles, since the grain growth might have been incomplete at 300 °C. The 100 nm size secondary particle were derived from inter-agglomerate densification [25]. It has to be mentioned that water content in the reverse micelles system can results in aggregation of the particles.

3.3. FT-IR Analysis

The FT-IR spectra are shown in Figure 5. The absorption peaks at 3370-3525 cm^{-1} and 1623 cm^{-1} were corresponding to stretching vibrations of the −OH and bending vibrations of the adsorbed water molecules, respectively. The main transmittance peak at 616.3 cm^{-1} was assigned to the Ti−O and Ti−O−Ti bonds. Bands at about 1170 cm^{-1} and 1650 cm^{-1} were assigned to carbon-related contaminants such as Ti–O–C and adsorbed water, respectively [26]. The FT-IR spectrum exhibited the peak at 644cm^{-1} for C−C bond vibration, 780 cm^{-1} for C−H stretching vibration for aromatic compounds and 1620 cm^{-1} for C=C aromatic stretching vibration. These banding vibration were detected due to residual carbon-related contaminants because of surfactant and oil. Fe doping FT-IR shows the peak at 1639 cm^{-1} and 3200 cm^{-1} because of −OH bending and stretching vibration of OH groups. The 537 cm^{-1} band was related to the Ti−O stretching vibrating which has been shifted to the lower wavelength by the introduction of Fe^{3+} ions. The FT-IR spectra of Fe−TiO_2 do not show any band corresponding to the Fe=O bonding. It may be due to this reason that the content of the incorporated Fe is slight. Also, the bending frequency of the Fe−O bonding might be overlapped with the Ti−O bonding frequency below 850 cm^{-1}. Therefore, overlapped peaks were observed in this region. Ni doping revealed that the peaks at 3421, 2804, and 1263 cm^{-1} were attributable to C−H bond stretching, whereas the peaks at 1263, 899, and 807 cm^{-1} were attributable to the C−H vibration band and C−H bending (out of plane), respectively [27-29].

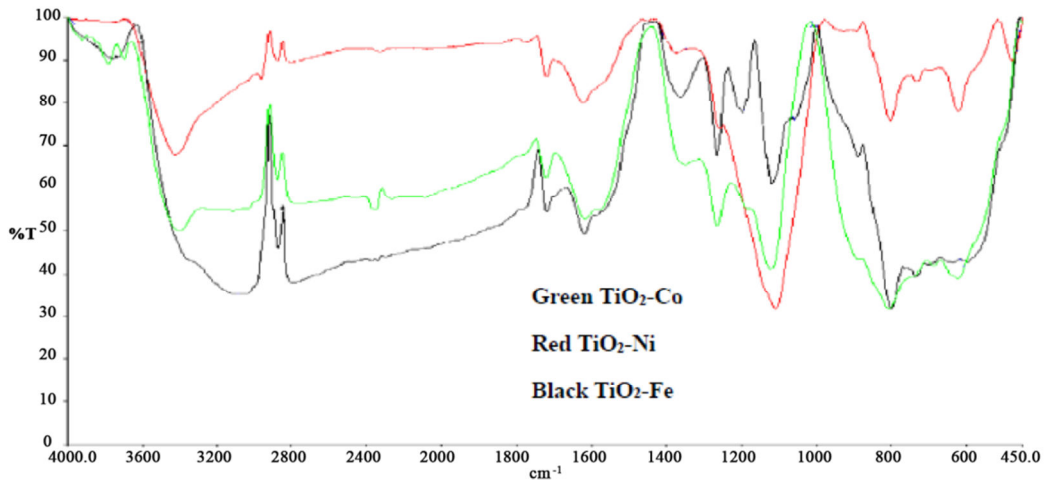

Figure 5: FT-IR spectra of TiO_2-Fe, TiO_2-Ni and TiO_2-Co.

3.4. Effect of pH

The effect of pH on the ability of products for decolorization of dyes was studied by changing pH in the range of 3-8. As shown in Figure 6, pH can be effective on decolorization of dyes in the presence of the as-prepared products (M-doped TiO_2 (M = Fe, Co and Ni) nanostructures). Herein, T = 25 °C, reaction time = 80 min, dosage of dopants = 0.03 g, and pH of solution was adjusted by HCl and/or NaOH. According to Figure 7, decreasing the pH values of solution increases the decolorization percentage, so the best efficiency is observed at pH = 3. The isoelectric point of TiO_2 is 6.6, so TiO_2 surface will be positively charged in lower pH [30] and will be negatively charged due to adsorption of OH^- on TiO_2 surface in higher pH. So, the decolorization efficiency increases in the acidic condition (pH < 7), and decreases in alkaline condition (pH > 7). Since the dye molecules having sulfonic groups (SO^{3-}) are negatively charged it is possible that the electrostatic attraction occurs between the positively charged catalyst surface and color molecules in acidic condition, whilethe electrostatic repulsion occurs between the dye and the negatively charged catalyst in alkaline condition [30].

3.5. Effect of TiO_2 content on decolorization process

The effect of photocatalyst dosage on decolorization efficiency was investigated by using various amounts (0.01 to 0.04 g) of M-doped TiO_2 (M = Fe, Co and Ni) nanostructures as photocatalyst. As shown in Figure 7, increasing the photocatalyst to a certain amount increases the decolorization efficiency, butthe rate of photocatalytic reaction and decolorization efficiency decrease by further increasing the TiO_2 content. So, the optimum amount of photocatalyst should be chosen to achieve the highest efficiency of decolorization [30, 31]. Herein, 0.03 g of M-doped TiO_2 (M = Fe, Co and Ni) nanostructures was considered as optimum amount.

3.6. Kinetics of decolorization

By considering the obtained results, it can be said that photocatalytic reaction follows the pseudo first-order kinetic model. A modified Langmuir–Hinshelwood (L–H) was adopted to rationalize the dye degradation kinetics. The equation is given below:

$$-\frac{dC}{dt}=\frac{k_T k_e C}{1+k_e C} \tag{2}$$

where k_T is the apparent reaction rate constant, k_e is the apparent equilibrium constant for the adsorption of the dye onto illuminated photocatalyst and C is the dye concentration at time t (mg/L).

The integrated form of Eq. (2) is given as below:

$$t=\frac{1}{k_e k_T}\ln\frac{C_0}{C}+\frac{1}{k_T}(C_0-C) \tag{3}$$

where C_0 and C are the initial dye concentration (mg/L) and dye concentration at time t (mg/L), t is reaction time (min) and k′ is the first-order rate constant (min^{-1}) [32, 33]. In Figure 8, the values of *k*

and R^2 (correlation coefficient) of dye decolorization by M-doped TiO_2 (M = Fe, Co and Ni) nanostructures are shown in Table 2. Linear relationship with the correlation coefficient R^2 for 0.9 in 20 mg/L concentration was shown. On the other hand, decreasing the rate constant of dye decolorization reaction by increasing the dye concentration indicated that the decolorization reaction follows the first-order kinetics. According to Figure 8, M-doped TiO_2 (M = Fe, Co and Ni) nanostructures have higher initial rate and catalytic activity. So, decolorization of dyes was done in existence of them, quickly. The reduced rate of reaction decreased after 80 min, this is induced by following the kinetics of reactions from pseudo-first-order [32].

3.7. Photocatalytic decolorization in the presence of daylight lamp

After optimizing the parameters such as pH and concentration of photocatalyst for the decolorization of dye under UV lamp in the batch reactor, decolorization of A.B.74 was also studied under daylight lamp in the batch reactor. The degradation of A.B.74 solution under a daylight lamp is illustrated in Figure 9.

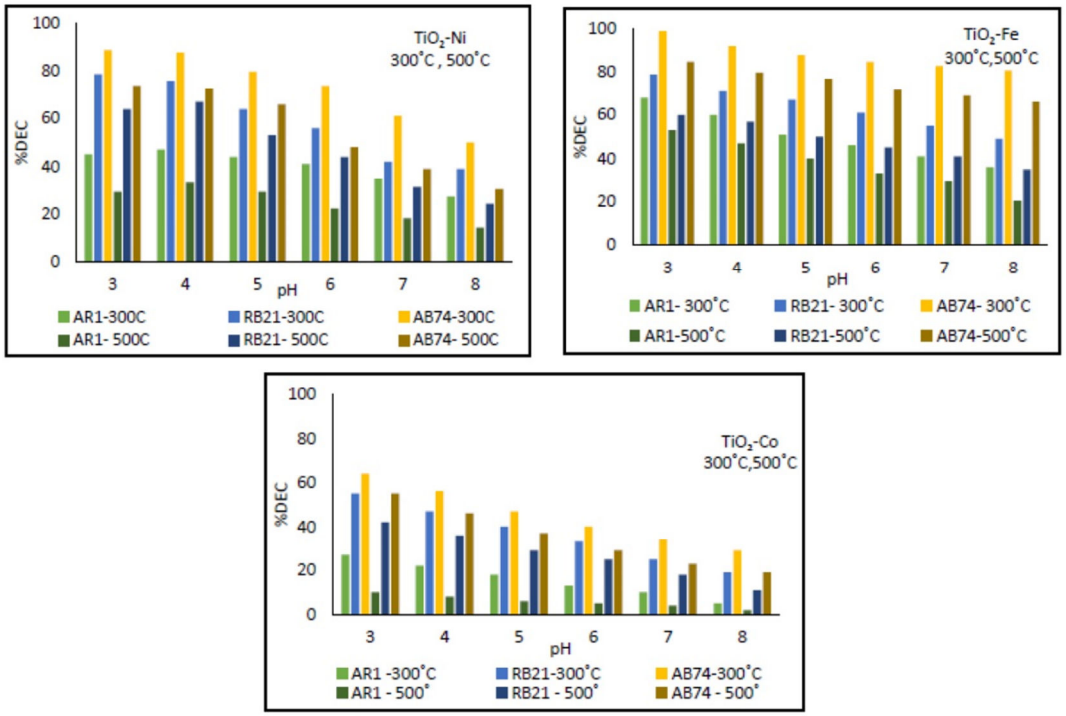

Figure 6: Effect of pH on photo-degradation efficiency of A.R.1, R.B.21, A.B.74, C= 20 mL, $Dosage_{TiO2}$= 0.03 g, V=1000 mL, T=25 °C.

Table 2: The characterization of the synthesized photocatalyst nanoparticles.

Photocatalyst	Formula	Code
Iron doped titania	$1TiO_2$-0.02 Fe	TiO_2-Fe (300,500)
Cobalt doped titania	$1TiO_2$-0.02 Co	TiO_2-Co (300,500)
Nickel doped titania	$1TiO_2$-0.02 Ni	TiO_2-Ni (300,500)

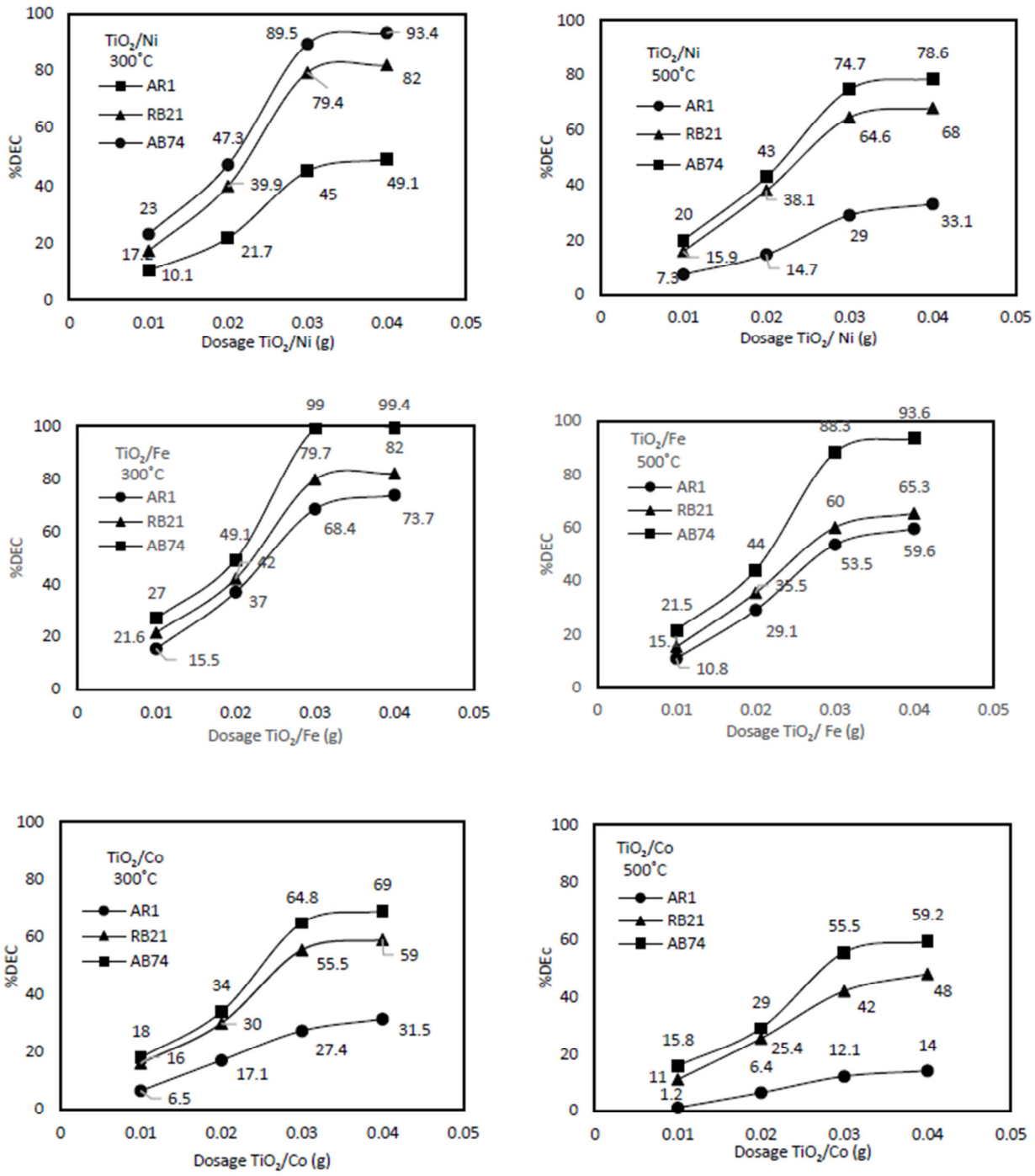

Figure 7: Effect of Dosage doping TiO_2 on photo-degradation efficiency of A.R.1, R.B.21, A.B.74, C= 20 mL, V=1000 mL, T=25 °C.

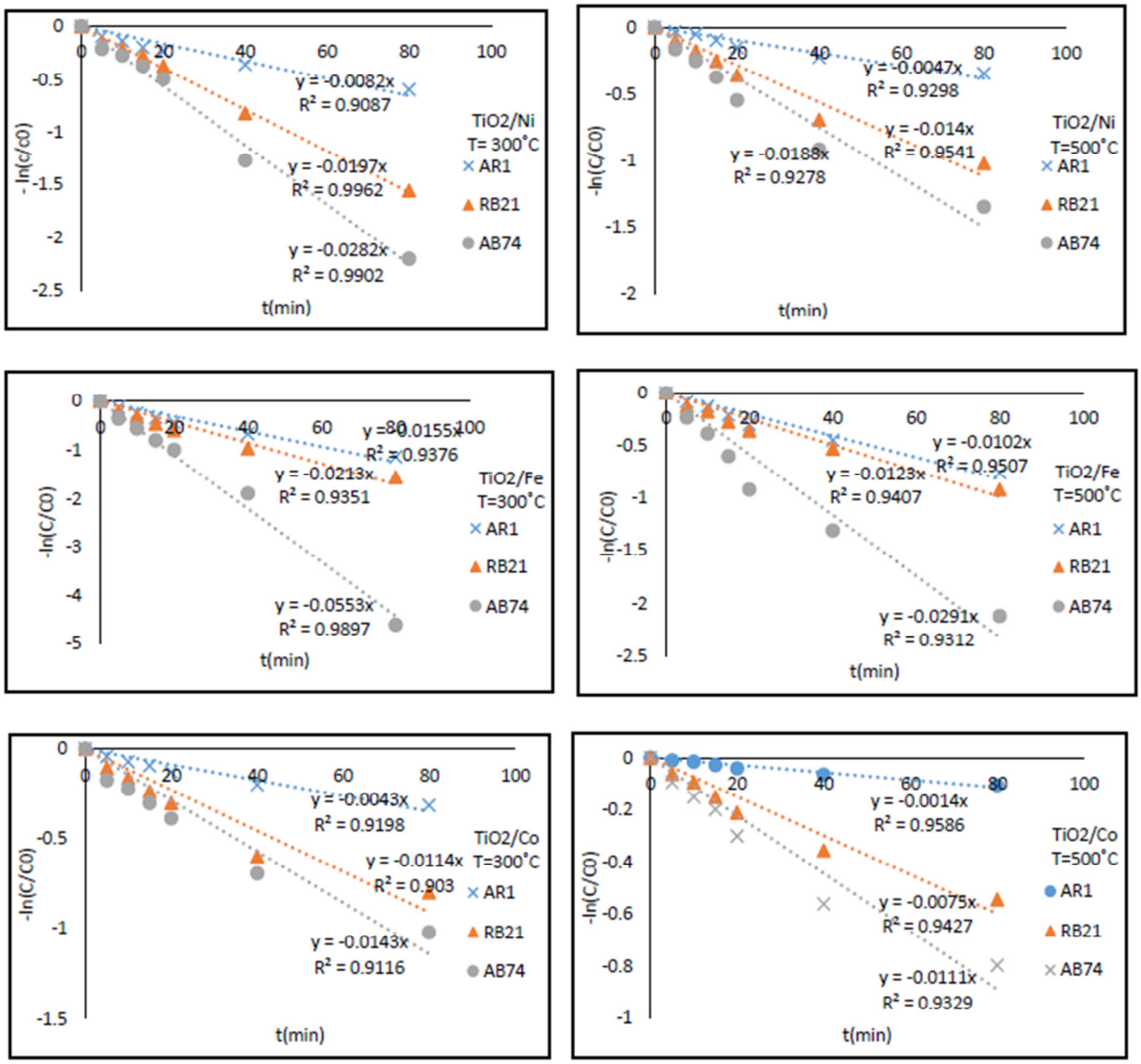

Figure 8. Pseudo First-order plots of photocatalytic decolorization of dyes under UV lamp.

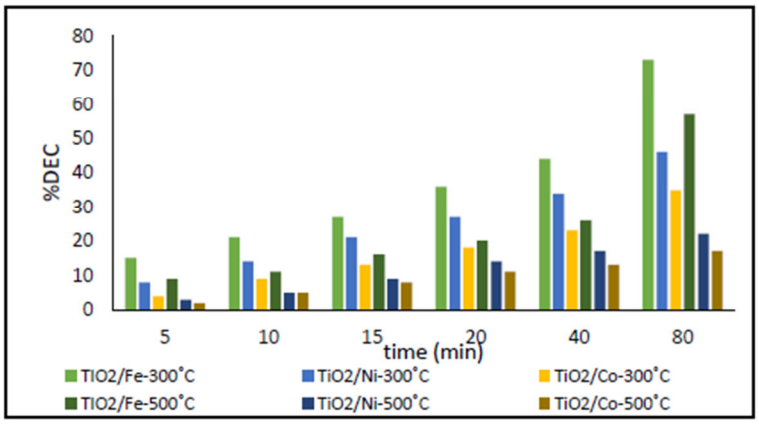

Figure 9: Decolorization efficiency of A.B.74 under daylight, C= 20 mL, DosageTiO_2= 0.03 g, V=1000 mL, T=25 °C.

As shown, the existence of Ni, Fe, and Co as dopants in TiO_2 lattice can increase the photocatalytic activity under visible irradiation (day-light lamp) by decreasing the band gap of pure TiO_2 [34]. As shown in Figure 10, the reaction kinetics of decolorization of the dye under day light lamp also followed the pseudo First-order kinetic model [13, 32].

3.8. Mechanism

The obtained results showed that M-doped TiO_2 (M = Fe, Co and Ni) can be considered as effective photocatalysts under UV and day light irradiation. As shown in Scheme 1, substitution of Fe, Ni and Co as dopants with Ti in TiO_2 lattice can decrease the band gap of TiO_2 by creating the secondary levels, so photocatalytic activity of M-doped TiO_2 increases under visible irradiation [35].

When a photocatalyst is exposed to irradiation, electron-hole pairs are formed and the excited electrons are transferred to the conduction band (CB), but the holes (h^+) remain in valence band (VB). Electrons and holes are active agents for photocatalytic activities, but the recombination of electron-hole pairs occurs quickly, so decreasesthe photocatalytic activity. Doping retards therecombination of the electron-hole pairs, hence increasingtheir activities.

In general, the metal could enhance photocatalytic activity of TiO_2 by creating a Schottky junction between metal and semiconductor. The metal particle acts as a sink for photo-generated electrons, so the rate of recombination process decreases and the photocatalytic activity increases [35, 36] (Scheme 1).
In this work, Fe, Ni and Co metals were used as dopants in TiO_2 lattice. The photocatalytic activity of the TiO_2 doped with these metals was better than pure TiO_2 under UV and daylight irradiation. It can be said that the separation of electrons and holes occurs due to the trapping of electrons [35-37]. The holes can scavenge surface adsorbed water or hydroxyl molecules, generating highly reactive hydroxyl radical species. On the other hand, scavenging oxygen molecules are very reactive superoxide radicals [35].

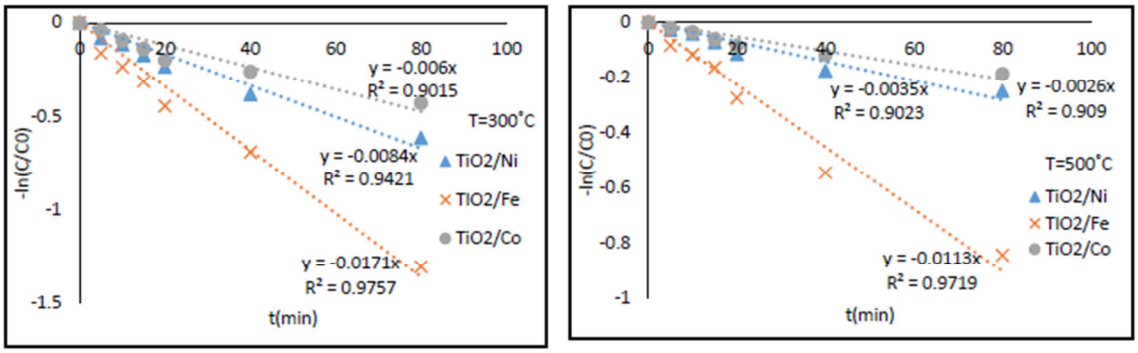

Figure 10: Pseudo First-order plots of photocatalytic decolorization of dyes under day light.

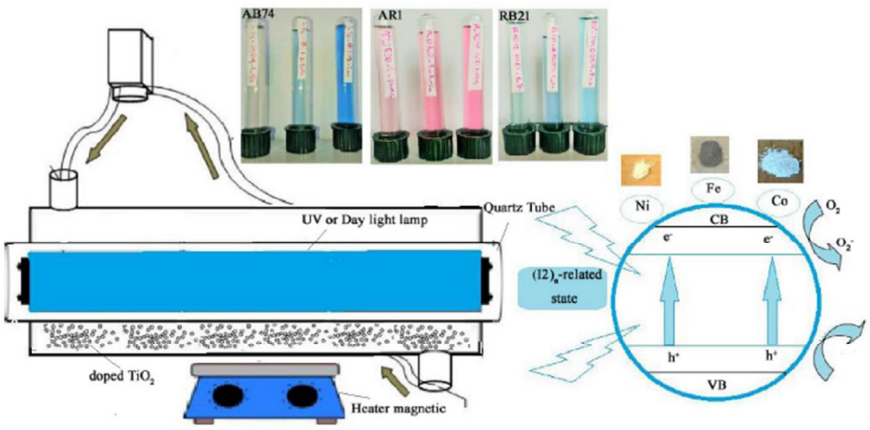

Scheme 1: The Proposed photocatalytic mechanism for M-doped TiO_2 (M = Fe, Ni and Co) photocatalyst under UV and daylight.

4. Conclusions

In this paper, M-doped TiO_2 nanostructures (M = Fe, Co and Ni) were synthesized by reverse microemulsion method. The decolorization ability of the as-prepared products under UV and visible irradiation was investigated using three dyes: Acid Red 1 (A.R.1), Reactive Blue 21 (R.B.21) and Indigo Carmine (A.B.74). The results showed that TiO_2 doped with Fe, Ni and Co presents better photocatalytic performance than pure TiO_2 under UV and visible irradiation. The photocatalytic performance improved due to the presence of dopants which can create inhibitors for electron-hole recombination. On the other hand, the dopants can decrease the band gap of TiO_2 through the secondary levels that are formed by substituting dopants with Ti in TiO_2 lattice, so the photocatalytic activity of TiO_2 will be increased under visible irradiation. The investigation illustrated that the photocatalytic reactions follow the pseudo First-order kinetic model and the Langmuir-Hinshelwood mechanism. Generally, maximum and minimum photocatalytic activities were observed for the Fe-TiO_2 (calcined at 300˚C) for degradation of A.B.74 dye and for Co-TiO_2 (calcined at 500˚C) for degradation of A.R.1 dye, respectively.

Acknowledgements

The authors are grateful to Council of Institute for Colorants, Paint and Coatings-ICST, Tehran, Iran, for providing financial support to undertake this work.

Conflict of interest

The authors (have received research grant from the Council of Institute for Colorants, Paint and Coatings-ICST, Tehran, Iran.

5. References

1. N. Naciri, A. Farahi, S. Rafqah, H. Nasrellah, M.A. El Mhammedi, I. Lançar, M. Bakasse, Effective photocatalytic decolorization of indigo carmine dye in Moroccan natural phosphate–TiO_2 aqueous suspensions, *Opti. Mater.*, 52(2016) 38-43.
2. F.P. VanderZee, S. Villaverde, Combined anaerobic–aerobic treatment of azo dyes—a short review of bioreactor studies, *Water Res.*, 39(2005) 1425-1440.
3. N.M. Mahmoodi, Z. Mokhtari-Shourijeh, Preparation of aminated nanoporous nanofiber by solvent casting/porogen leaching technique and dye adsorption modeling, *J. Taiwan Inst. Chem. Eng.*, 65 (2016) 378-389.
4. P. Abdi, A. Farzi, A. Karimi, Application of a hybrid enzymatic and photo-fenton process for investigation of azo dye decolorization on TiO_2/metal-foam catalyst, *J. Taiwan Inst. Chem. Eng.*, 71(2016), 137-144.
5. M. Salavati-Niasari, F. Soofivand, A. Sobhani-Nasab, M. Shakouri-Arani, A.Y. Faal, S. Bagheri, Synthesis, characterization, and morphological control of $ZnTiO_3$ nanoparticles through sol-gel processes and its photocatalyst application, *Adv. Powder Technol*, 27(2016), 2066-2071.
6. F. Soofivand, M. Sabet, H. Seyghalkar, M. Salavati-Niasari, Using the [Co $(oct)_2$] as a New Precursor for Simple Synthesis of CoS_2 Nanoparticles and Kinetics Studies on Photocatalytic Activities Under UV Irradiation, *J. Nanostruct.*, 8(2018) 75-81.
7. F. Soofivand, M. Salavati-Niasari, Co_3O_4/graphene nanocomposite: pre-graphenization synthesis and photocatalytic investigation of various magnetic nanostructures, *RSC Adv.*, 5(2015), 64346-64353.
8. F. Soofivand, M. Salavati-Niasari, Step synthesis and photocatalytic activity of NiO/graphene nanocomposite under UV and visible light as an effective photocatalyst, *J. Photochem. Photobiol. A: Chem.*, 337(2017), 44-53.
9. O.K. Varghese, D. Gong, M. Paulose, K.G. Ong, E.C. Dickey, C.A. Grimes, Extreme changes in the electrical resistance of titania nanotubes with hydrogen exposure, *Adv. Mater.*, 15(2003), 624-627.
10. S. Livraghi, A. Votta, M.C. Paganini, E. Giamello, The nature of paramagnetic species in nitrogen doped TiO_2 active in visible light photocatalysis, *Chem. Commun.*, (2005), 498-500.
11. S. Ikezawa, H. Homyara, T. Kubota, R. Suzuki, S. Koh, F. Mutuga, T. Yoshioka, A. Nishiwaki, Y. Ninomiya, M. Takahashi, Applications of TiO_2 film for environmental purification deposited by controlled electron beam-excited plasma, *Thin Solid Films*, 386(2001), 173-176.
12. K. Seyyedi, M.A.F. Jahromi, Decolorization of Azo Dye CI Direct Black 38 by Photocatalytic Method Using TiO_2 and Optimizing of Process, *APCBEE Proced.*, 10(2014), 115-119.
13. M. Pelaez, N.T. Nolan, S.C. Pillai, M.K. Seery, P. Falaras, A.G. Kontos, P.S. Dunlop, J.W. Hamilton, J.A. Byrne, K. O'shea, A review on the visible light active titanium dioxide photocatalysts for environmental applications, *Appl. Catal. B: Environ.*, 125(2012), 331-349.
14. M. Ahmed, Synthesis and structural features of mesoporous NiO/TiO_2 nanocomposites prepared by sol–gel method for photodegradation of methylene blue dye, *J. Photochem. Photobiol. A: Chem.*, 238(2012), 63-70.
15. M. Ahmed, E.E. El-Katori, Z.H. Gharni, Photocatalytic degradation of methylene blue dye using Fe_2O_3/TiO_2

nanoparticles prepared by sol–gel method, *J. Alloy Compoun.*, 553(2013), 19-29.
16. G. Zhu, K. Zhou, Preparation and characterization of nitrogen-doped titanium dioxides, *Sci. China Series B: Chem.*, 50(2007), 212-216.
17. G. Mei Li, Z. Xiao-Dong, L. Chun-Tian, J. Guo-Zhi, Mechanism of visible photoactivity of F-doped TiO_2, *Chinese Phy. Lett.*, 27(2010), 057103.
18. A. Ranjitha, N. Muthukumarasamy, M. Thambidurai, D. Velauthapillai, R. Balasundaraprabhu, S. Agilan, Fabrication of Ni-doped TiO_2 thin film photoelectrode for solar cells, *Sol. Energy*, 106(2014), 159-165.
19. C. Zhao, X. Shu, D. Zhu, S. Wei, Y. Wang, M. Tu, W. Gao, High visible light photocatalytic property of Co^{2+}-doped TiO_2 nanoparticles with mixed phases, *Super. Microstruct.*, 88(2015), 32-42.
20. V.K. Gupta, T. Eren, N. Atar, M.L. Yola, C. Parlak, H. Karimi-Maleh, $CoFe_2O_4$@ TiO_2 decorated reduced graphene oxide nanocomposite for photocatalytic degradation of chlorpyrifos, *J. Mol. Liquid*, 208(2015), 122-129.
21. B.M. Almeida, M.A. MeloJr, J. Bettini, J.E. Benedetti, A.F. Nogueira, A novel nanocomposite based on TiO_2/Cu_2O/reduced graphene oxide with enhanced solar-light-driven photocatalytic activity, *Appl. Surface Sci.*, 324(2015), 419-431.
22. M.H. Zori, Synthesis of TiO_2 nanoparticles by microemulsion/heat treated method and photodegradation of methylene blue, *J. Inorg. Organometall. Poly. Mater.*, 21(2011), 81-90.
23. M. Olya, M. Vafaee, M. Jahangiri, Modeling of acid dye decolorization by TiO_2–Ag_2O nano-photocatalytic process using response surface methodology, *J. Saudi Chem. Soc.*, (2015).
24. Y. Huang, W. Ho, Z. Ai, X. Song, L. Zhang, S. Lee, Aerosol-assisted flow synthesis of B-doped, Ni-doped and B–Ni-codoped TiO_2 solid and hollow microspheres for photocatalytic removal of NO, *Appl. Catalysis B: Environ.*, 89(2009), 398-405.
25. M. Karbassi, A. Nemati, M.H. Zari, K. Ahadi, Effect of Iron Oxide and Silica Doping on Microstructure, Bandgap and Photocatalytic Properties of Titania by Water-in-Oil Microemulsion Technique, *Transact. Indian Ceramic Soc.*, 70 (2011), 227-232.
26. E.C. Ilinoiu, R. Pode, F. Manea, L.A. Colar, A. Jakab, C. Orha, C. Ratiu, C. Lazau, P. Sfarloaga, Photocatalytic activity of a nitrogen-doped TiO_2 modified zeolite in the degradation of Reactive Yellow 125 azo dye, *J. Taiwan Instit. Chem. Eng.*, 44(2013), 270-278.
27. Z. Mesgari, M. Gharagozlou, A. Khosravi, K. Gharanjig, Synthesis, characterization and evaluation of efficiency of new hybrid Pc/Fe-TiO_2 nanocomposite as photocatalyst for decolorization of methyl orange using visible light irradiation, *App. Catalysis A: General*, 411(2012), 139-145.
28. C. Sahoo, A.K. Gupta, Characterization and photocatalytic performance evaluation of various metal ion-doped microstructured TiO_2 under UV and visible light, *J. Environ. Sci. Health, Part A*, 50(2015), 659-668.
29. J. Kamalakkannan, V. Chandraboss, S. Prabha, S. Senthilvelan, Activated Carbon Loaded N, S co-doped TiO_2 Nanomaterial and Its Dye Wastewater Treatment, *Inter. Lett. Chem. Phy. Astron.*, 47(2015), 147-164.
30. K. Seyyedi, M.A.F. Jahromi, Decolorization of Azo Dye CI Direct Black 38 by Photocatalytic Method Using TiO_2 and Optimizing of Process, *APCBEE Procedia*, 10(2014), 115-119.
31. Z. Abou-Gamra, M. Ahmed, Synthesis of mesoporous TiO_2–curcumin nanoparticles for photocatalytic degradation of methylene blue dye, *J. Photochem. Photobiol. B: Biology*, 160(2016), 134-141.
32. R.L. Narayana, M. Matheswaran, A.A. Aziz, P. Saravanan, Photocatalytic decolourization of basic green dye by pure and Fe, Co doped TiO_2 under daylight illumination, *Desalination*, 269(2011), 249-253.
33. M. Sundararajan, V. Sailaja, L.J. Kennedy, J.J. Vijaya, Photocatalytic degradation of rhodamine B under visible light using nanostructured zinc doped cobalt ferrite: Kinetics and mechanism, *Ceramics Internat.*, 43(2017), 540-548.
34. H. Moradi, A. Eshaghi, S.R. Hosseini, K. Ghani, Fabrication of Fe-doped TiO 2 nanoparticles and investigation of photocatalytic decolorization of reactive red 198 under visible light irradiation, *Ultrason. Sonochem.*, 32(2016), 314-319.
35. D. Wang, J. Li, G. Zhou, W. Wang, X. Zhang, X. Pan, Low Temperature Hydrothermal Synthesis of Visible-Light-Activated I-Doped TiO_2 for Improved Dye Degradation, *J. Nanosci. Nanotechnol.*, 16(2016), 5676-5682.
36. A.T. Kuvarega, R.W. Krause, B.B. Mamba, Nitrogen/palladium-codoped TiO_2 for efficient visible light photocatalytic dye degradation, *J. Phy. Chem. C*, 115(2011), 22110-22120.
37. M.Y. Xie, K.Y. Su, X.-Y. Peng, R.J. Wu, M. Chavali, W.C. Chang, Hydrogen production by photocatalytic water-splitting on Pt-doped TiO_2–ZnO under visible light, *J. Taiwan Instit. Chem. Eng.*, 70(2017), 161-167.

How to cite this article:
M. Hosseini-Zori, Z. Mokhtari shourijeh, Synthesis, Characterization and Investigation of Photocatalytic Activity of Transition Metal-doped TiO_2 Nanostructures. Prog. Color Colorants Coat., 11 (2018), 209-220.